Hindawi Publishing Corporation
Shock and Vibration
Volume 2015, Article ID 265321, 15 pages
http://dx.doi.org/10.1155/2015/265321

Review Article

Theoretical Research Progress in High-Velocity/Hypervelocity Impact on Semi-Infinite Targets

Yunhou Sun,[1,2] Cuncheng Shi,[1,3] Zheng Liu,[1] and Desheng Wen[1]

[1] *State Key Laboratory for Disaster Prevention & Mitigation of Explosion & Impact, PLA University of Science and Technology, Nanjing 210007, China*
[2] *Beijing Canbao Architecture Design Institute, Beijing 100036, China*
[3] *The Fifth Department, 145 Erqi Road, Wuhan 430012, China*

Correspondence should be addressed to Yunhou Sun; houyunsun@126.com

Received 3 November 2014; Revised 2 February 2015; Accepted 5 February 2015

Academic Editor: Mohammad Elahinia

With the hypervelocity kinetic weapon and hypersonic cruise missiles research projects being carried out, the damage mechanism for high-velocity/hypervelocity projectile impact on semi-infinite targets has become the research keystone in impact dynamics. Theoretical research progress in high-velocity/hypervelocity impact on semi-infinite targets was reviewed in this paper. The evaluation methods for critical velocity of high-velocity and hypervelocity impact were summarized. The crater shape, crater scaling laws and empirical formulae, and simplified analysis models of crater parameters for spherical projectiles impact on semi-infinite targets were reviewed, so were the long rod penetration state differentiation, penetration depth calculation models for the semifluid, and deformed long rod projectiles. Finally, some research proposals were given for further study.

1. Introduction

In the 1950s, under the motivation of aerospace exploration and weapon design, high-velocity/hypervelocity impact phenomena gradually became a hot topic. Kinslow (1970) wrote a book entitled *High Velocity Impact Phenomena* [1] which systematically summarized the research progress of this topic. After the USA Landing Moon Plan being successfully carried out and the Missile Shield Plans termination, the research entered into a declinable period. It was not until the Strategic Defense Initiative (SDI) was presented in 1983 that the research received attention again. Herrmann and Wilbeck (1987) [2] reviewed the hypervelocity penetration theories. Zhang and Huang [3] wrote a book entitled *Hypervelocity Impact Dynamics Introduction* in which the phases transition, equation of state, penetration in different conditions, and hypervelocity emission technology were systematically introduced. In recent years, with the progress of hypervelocity weapon research, the damage mechanism has received more and more attention [4]. This paper will summarize the research progress in high-velocity/hypervelocity impact on semi-infinite targets, including the impact velocity regions, spherical projectile crater effect on semi-infinite targets, and long rod projectile penetration theories, and give some proposals for future research.

2. Impact Velocity Regions

High-velocity/hypervelocity impact is a course with huge energy releasing, high temperature, and pressure. The increase of entropy due to the strong shock wave is enough to lead to materials structures change, damage and even meltingness, vaporization, and ionization [5]. For a certain projectile-target group, velocity is the only factor for determining impact effect and its change brings different damage mechanisms of materials. Therefore, impact velocity region determination is one of the basic problems in high-velocity/hypervelocity impact.

2.1. High-Velocity Lower Limit. If the dynamic pressure is lower than the dynamic yield strength, the material is elastic.

Table 1: Impact phenomena classification and state evaluation.

Impact velocity	Phenomena	$\rho_t u^2/Y_t$	Material state
<0.05 km/s	Majority is elastic	10^{-5}	Quasi-elastic-plastic
0.05~0.5 km/s	Majority is plastic	10^{-3}	plastic deformation appears
0.5~1 km/s	Viscosity and intensity are remarkable	10^{-1}	Plastic
1~3 km/s	Material changes from plastic to fluid with strength	10	Remarkable plastic
3~12 km/s	Fluid	10^{3}	Liquid
>12 km/s	Vaporization happens		

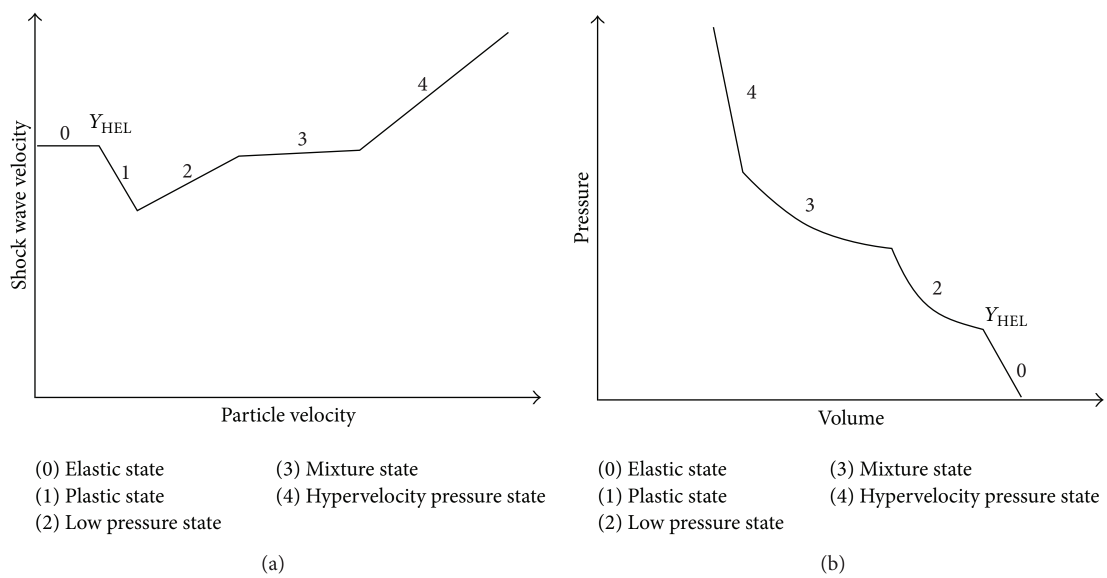

Figure 1: Material responses under different pressures [6].

With dynamic pressure increase the material enters into the plastic state and quasifluid state as 2-3-4 in Figure 1 [6]. In elastic and plastic states, the material strength plays an important role, while in quasifluid state the compressibility does. So it is reasonable to regard the quasifluid state as the high-velocity penetration region and the state that compressibility takes an obvious leading position as the hypervelocity penetration one.

Based on experiments of metals, Weirauch [7] proposed a classification method (Table 1) with the dimensionless parameter $\rho_t u^2/Y_t$ (where ρ_t is target material density, u is the impact velocity, and Y_t is the strength parameter of target material) to evaluate impact patterns. Though it describes material characters well, the meaning and value of Y_t are not clear. Jing [8] suggested that if $P \geq a_t\sigma_{yt}$ (P is the pressure, σ_{yt} is the dynamic yield strength, and a_t is the constant which shows the relationship between P and σ_{yt}, $8 < a_t \leq 10$), 1D-strain curve is very close to the hydrostatic pressure curve and material could be looked as fluid. Additionally, Walters and Zukas [9] took the velocity corresponding to the pressure $P = 10\sigma_{yt}$ (where σ_{yt} is the dynamic yield stress) as the critical value and solved penetration problems by Bernoulli equation without considering the strength effect of target. Based on the requirements of Jing [8] and Walters and Zukas [9], the following equation can be obtained:

$$u > \sqrt{\frac{2a_t\sigma_{yt}}{\rho_t}}, \quad 8 < a_t \leq 10. \tag{1}$$

Walker [10] found that if the expansion speed of cavity is larger than $0.2c_0$ (c_0 is the bulk sound speed), the target strength can be neglected. Qian and Wang [11] found that if the cavity-expansion speed is larger than $0.2c_L$ (c_L is the longitudinal wave speed), the target material would enter into quasifluid state.

Fomin et al. [5] advised that if the errors between theoretical calculating results and the average values of experiments are less than 10%, target material strength can be neglected and the corresponding value of critical velocity is equal to $3\sqrt{H_t/\rho_t}$ (H_t is the material dynamic hardness and is equal to the specific plastic deformation work, $H_t = 3\sigma_{yt}$) and the following equation is obtained

$$u > \sqrt{\frac{27\sigma_{yt}}{\rho_t}}. \tag{2}$$

The critical velocities of different materials neglecting the strength from different methods are shown in Table 2. It

Table 2: The critical velocity ignoring the target material strength.

Materials	ρ_t g/cm^3	K GPa	ν	σ_{yt} GPa	(1) m/s	$0.2c_L$ m/s	$0.2c_0$ m/s	(2) m/s
Tungsten alloy [74]	17.3	291.7	0.3	2.4	1490–1666	1046	821	645
Steel 4340 [42, 43, 74]	7.85	170.8	0.3	1.978	2008–2245	1186	932	869
Aluminum alloy 6061 [42, 43, 74]	2.71	67.65	0.33	0.625	1929–2148	1228	999	832
Concrete [103]	2.4	15.625	0.18	0.0619	643–718	736	510	278
Granite [104]	2.67	36.87	0.16	0.1822	1045–1168	1095	743	452

can be seen that the results of different methods have great differences. The results of concrete and granite from (1) and $0.2c_L$ are coincident, while those from (2) and $0.2c_0$ are not. The difference of (2) is due to the premise that the errors should be within 10%. If the error value is smaller, the results from (2) and $0.2c_0$ would be closer to those from (1) and $0.2c_L$. Above all, it is reasonable to consider the quasifluid velocity as the critical value of high-velocity penetration.

2.2. Hypervelocity Lower Limit. At present, most of documents [2, 3] defined the velocity that semispherical crater appears as hypervelocity according to experimental phenomena. Jonas and Zukas [12] suggested that the compressibility could not be neglected if the impact velocity is 3~12 km/s. However, it is only a rough evaluation. Jing [13] regarded the value corresponding to atomization appearance as the boundary of hypervelocity. Fomin et al. [5] found that, when Mach number $M_0 = v_0/c_0$ (v_0 and c_0 are the impact velocity and material sonic speed, resp.) is closed to 0.75, target material would be damaged and even phase states transformation and some explosion properties appear. Wang [14] introduced Mach number and considered the impact velocity and the temperature and pressure change and used Bridgman equation of state

$$\frac{\Delta V}{V_0} = -A\tilde{p} + B\tilde{p}, \tag{3}$$

where $\tilde{p} = p/p_0$, V_0 and p_0 are initial volume and pressure, respectively, p is hydrostatic pressure, and ΔV is the volume change results from p. A and B are the coefficients depending on temperature. If M_0 is greater than 0.75, the hydrostatic pressure p would be much greater than the shear stress component, which means that the compression deviates the linear rule and enters into phases transition region and the compressibility occupies the leading position. It is reasonable to regard $0.75c_0$ as the critical velocity for hypervelocity impact. In fact, if the velocity is larger than $0.75c_0$, there are microwave spectrum, infrared spectrum, visible spectrum, ultraviolet ray spectrum, and electromagnetic radiation ionization [5] with the velocity increasing, so the region could be divided into many secondary regions further. The evaluation methods for hypervelocity impact of Wang and Jing are similar and they have physical bases and high suitability for regarding $0.75c_0$ as the critical value of hypervelocity impact.

Above all, the points that the strength could be neglected and the compressibility occupies the leading position are the two typical states, so it is reasonable to define high-velocity and hypervelocity impact regions with them. However, there are differences in the methods for determining critical value of high-velocity impact and this needs further research.

3. Crater Effect of Spherical Projectile Penetration into a Semi-Infinite Target

Spherical projectile penetration into semi-infinite target is a typical problem of high-velocity/hypervelocity impact. Besides obvious plastic deformation, there are also meltingness, vaporization, and ionization. It is difficult to describe the crater effect through introducing equation of state suitable for a wide-range pressure in theoretical models. Generally speaking, the impact progress can be divided into four regimes as Figure 2(a) shows [2]. Because the ratio of length to diameter is small, the projectile has been completely eroded in transient shock regime and steady state regime does not appear. The momentum field change in the target leads to cavitation as Figure 2(b) shows. Transient shock regime and cavitation regime form a complicated course, which increases the difficulty of theoretical research. Therefore, the researches on projectile penetration into semi-infinite target all focus on empirical formulae, and theoretical models are rare.

3.1. Crater Shape. Since the 1950s, researchers [15–22] carried out lots of semi-infinite targets high-velocity/hypervelocity impact experiments by the spherical projectiles. Most of the target materials are ductile metals such as aluminum, copper, steel, and Lead. The basic relationship between the crater shape and impact conditions was obtained. For impact on target of low strength and density by projectile with high strength and high density, the projectile kept intact and a deep-hole crater with a diameter a little greater than that of projectile is formed [2, 3]. If impact velocity is high enough, the projectile would deform and even get crushed, and the crater would change to another kind of shape and the crater depth decreases with impact velocity. This also appears for projectile with low strength and low density penetration into target of same material or the material with high strength and density [2, 3]. For higher impact velocity, projectiles crush in transient shock regime and craters are closed to semisphere as shown in Figure 3(a). So the semispherical crater is generally regarded as the typical state of hypervelocity impact [2, 3, 13]. For impact with the spherical projectile, the crater is semispherical for any projectile-target groups.

The semispherical crater theory received great challenges from many experiments. Stanyukovich [23] found that the crater could be flat with $P < D_c$ in the research on the vaporization characters of materials under high pressure. From

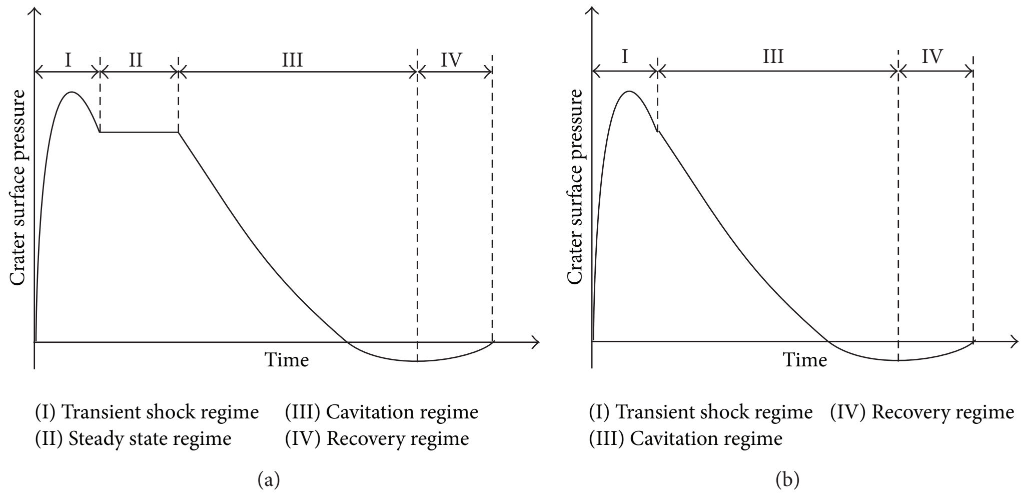

Figure 2: The crater surface pressure versus time.

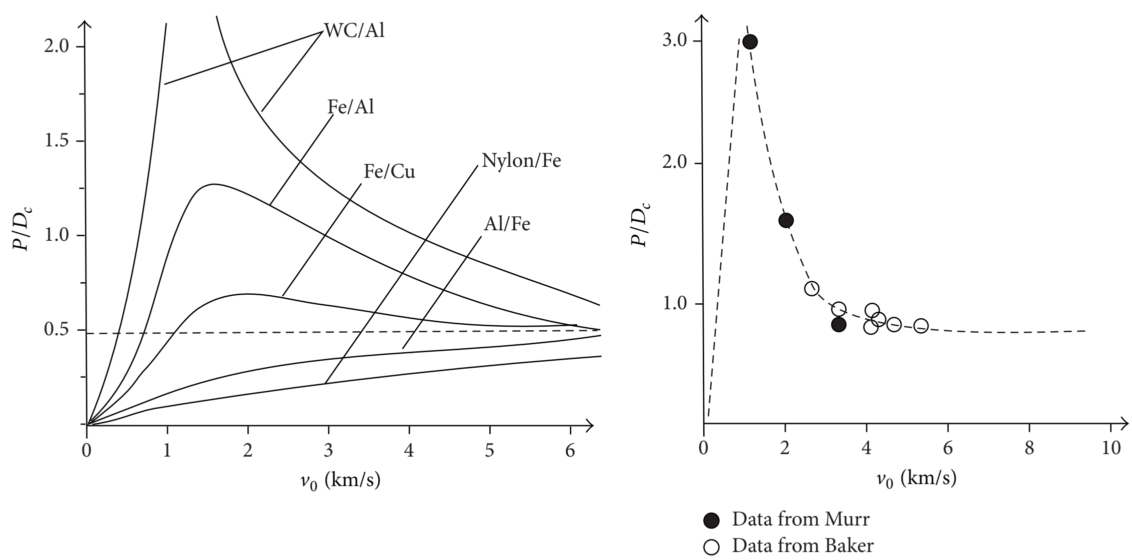

(a) [3, 13]

(b) [25, 26]

Figure 3: The relationship between crater shape and impact velocity for different projectile-target groups.

tungsten projectile hypervelocity impact on aluminum target experiments, Leontyev [24] found that when the impact velocity reaches 15 km/s, the crater shape changes from semispherical to flat. Murr et al. [25] and Baker [26] obtained a deep-hole crater whose depth is almost equal to the diameter (see Figure 3(b)) from aluminum target penetration experiments by stainless steel projectile, respectively. Yu et al. [27] pointed out that the semispherical crater is not applied to any case and proposed the symmetrical cavitation theory and regarded the symmetrical cavitation of the crater in all directions as the feature of hypervelocity impact. Based on the hypervelocity impact phenomena of rocks, Öpik [28], Gault [29], and Dence et al. [30] found that the crater diameter is greatly larger than depth and so are most of meteor craters. For example, meteor crater in Arizona is 1240 meters in diameter and 170 meters in depth [31].

Most of researches regarded that hypervelocity impact can form semispherical craters; however, the targets are metals and the impact velocities are less than 8 km/s, so the semispherical crater has no universal applicability. The crater shapes for projectiles impact on metal targets with larger velocity and high-velocity/hypervelocity impact on geologic materials still need to be studied further.

3.2. Crater Scaling Laws and Empirical Formulae. Impact crater is a complicated dynamic progress which involves density, strength, sonic speed, specific heat, melting point, and boiling point of both projectile and target materials. The crater diameter and depth are generally calculated with empirical formulae which are established by dimensional analysis from experimental data so far.

Zhang and Huang [3] chose projectile diameter (d_p), target density (ρ_t), and target strength (Y_t) as the three independent physical parameters, and dimensionless crater depth P and diameter D_c were obtained as follows:

$$\frac{P}{d_p} = f_1\left[\frac{v_0}{\sqrt{Y_t/\rho_t}}, \frac{\rho_p}{\rho_t}, \frac{Y_p}{Y_t}, \frac{c_p}{c_t}, \frac{(CT_m)_p}{(CT_m)_t}, \frac{n_p}{n_t}, \frac{(CT_v)_p}{(CT_v)_t}, \frac{n_t}{C_t^2}, \frac{(CT_v)_t}{n_t}, \frac{N_t}{N_p}, \frac{N_t}{C_t^2}\right], \quad (4a)$$

$$\frac{D_c}{d_p} = f_2\left[\frac{v_0}{\sqrt{Y_t/\rho_t}}, \frac{\rho_p}{\rho_t}, \frac{Y_p}{Y_t}, \frac{c_p}{c_t}, \frac{(CT_m)_p}{(CT_m)_t}, \frac{n_p}{n_t}, \frac{(CT_v)_p}{(CT_v)_t}, \frac{n_t}{C_t^2}, \frac{(CT_v)_t}{n_t}, \frac{N_t}{N_p}, \frac{N_t}{C_t^2}\right], \quad (4b)$$

where c is the bulk sound speed, C is the specific heat, T_m is the melting point, T_v is the boiling point, n is the melting heat, N is the boiling heat, and subscripts p and t denote projectile and target, respectively.

Westine and Mullin [32] discussed the effects of inertia, strength, compressibility, heating, liquefying, vaporization, and so on, and six dimensionless parameters were obtained as follows:

$$\pi_1 = \sqrt{\frac{\rho_t v_0^2}{Y_t}}, \quad \pi_2 = \frac{\rho_t C_r v_0^2}{Y_t}, \quad \pi_3 = \frac{\rho_t n_t}{Y_t},$$
$$\pi_4 = \sqrt{\frac{\rho_t c_t^2}{Y_t}}, \quad \pi_5 = \frac{\rho_t C_l T_v}{Y_t}, \quad \pi_6 = \frac{\rho_t N_t}{Y_t}, \quad (5)$$

where C_r and C_l are the target material specific heats corresponding to solid and liquid states, respectively. π_2/π_3 and π_4^3/π_3 could approximately be constants.

For the research at present, the proportions of melting and vaporization effects are little, and (4a)-(4b) can be expressed as

$$\frac{P}{d_p} = f_1\left[\frac{v_0}{\sqrt{Y_t/\rho_t}}, \frac{\rho_p}{\rho_t}, \frac{Y_p}{Y_t}, \frac{c_p}{c_t}, \frac{c_t}{v_0}\right], \quad (6a)$$

$$\frac{D_c}{d_p} = f_2\left[\frac{v_0}{\sqrt{Y_t/\rho_t}}, \frac{\rho_p}{\rho_t}, \frac{Y_p}{Y_t}, \frac{c_p}{c_t}, \frac{c_t}{v_0}\right], \quad (6b)$$

where $v_0/\sqrt{Y_t/\rho_t}$ is the relationship between the inertia and strength, ρ_p/ρ_t is the ratio of densities, Y_p/Y_t is the ratio of strengths, c_p/c_t is the ratio of bulk sound speeds, and c_t/v_0 is ratio of inertia and compressibility [33]. The fitting equation can be obtained from (6a)-(6b) and experimental data. Herrmann and Wilbeck [2] had summarized the empirical formulae obtained during 1958–1987. Yu et al. [27] proposed an empirical formula for the crater depth of metal target. These formulae can be expressed uniformly as

$$\frac{P}{d_p} = K_1\left(\frac{\rho_p}{\rho_t}\right)^m (v^*)^n, \quad (7)$$

where K_1, m, and n are the parameters obtained by experimental data fitting. The values of m, n, and dimensionless velocity v^* are shown in Table 3.

It can be seen from Table 3 that the main forms of dimensionless impact velocity v^* are $\sqrt{\rho_t v^2/H_B}$, $\sqrt{\rho_t v^2/H_t}$, $\sqrt{\rho_t v^2/Y_t}$, and v/c_t. The difference of v^* shows the different understandings for crater mechanism of hypervelocity impact. $\sqrt{\rho_t v^2/H_B}$, $\sqrt{\rho_t v^2/H_t}$, and $\sqrt{\rho_t v^2/Y_t}$ could be looked as the same form which highlights the importance of inertia and strength of target material, while v/c_t emphasizes the leading position of compressibility. From Figure 2(b), it can be known that the pressure peak at the impact moment can affect the crater progress and the plastic flow of materials in cavitation regime is controlled by inertia and strength. The empirical formulae with inertia, strength, and compressibility considered were established, and the representative ones are Sedgwick's, Xiang's, and Luo's equations.

Sedgwick's equation [34]:

$$\frac{P}{d_p} = 0.482\left(\frac{\rho_p}{\rho_t}\right)^{0.537}\left(\frac{v_0}{\sqrt{Y_t/\rho_t}}\right)^{0.47}\left(\frac{v_0}{c_t}\right)^{0.106}. \quad (8)$$

Xiang's equation [35]:

$$\frac{P}{d_p} = 0.37\left(\frac{v_0}{\sqrt{Y_t/\rho_t}}\right)^{0.56}\left(\frac{v_0}{c_t}\right)^{0.11}. \quad (9)$$

Luo's equation [36]:

$$\frac{P}{d_p} = 0.51\left(\frac{v_0}{\sqrt{Y_t/\rho_t}}\right)^{0.46}\left(\frac{v_0}{c_t}\right)^{0.20}. \quad (10)$$

From (8), (9), and (10), it can be found that the power's absolute values of Y_t (0.235, 0.28, and 0.23) are all greater than those of sonic speed c_t (0.106, 0.11, and 0.20). The ratios of power's absolute value of Y_t and c_t in Sedgwick's and Xiang's equations are both more than 2, which illustrates that the strength takes more important role in crater progress than compressibility. Yu et al. [27] pointed out that the transient shock regime is short, and the second regime in which density and strength occupy leading position lasts a longer time. So the density and strength are considered as the main parameters of affecting crater size. Additionally, most of the dimensionless impact velocity power is equal to or close to 2/3 which is the well-known 2/3 power law and is considered to be suitable to calculate crater depth by Yu et al. [27]. However, Baker [26] thought that the relationship between the crater diameter and impact velocity is not like (7) but linear. From Figure 4, it can be found that when impact velocity is less than 14 km/s the predicated results of the power function and linear function are similar; however, if impact velocity is larger than 14 km/s the results of them are different. So Baker thought that the linear relationship is more suitable to describe the crater effect for high-velocity impact than power functional relationship. Guo [37] also gave the same conclusion as Baker. Because their data samples are few and there is still uncertainty for the hypothesis that the crater

Table 3: The parameters value of (7).

Number	Authors	m	n	v^*	Remarks
1	Summers and Charters [15] (1958)	2/3	2/3	$v^* = v/c_t$	
2	Charters and Summers [105] (1959)	2/3	2/3	$v^* = \sqrt{\rho_t v^2/Y_t}$	
3	Herrmann and Jones [20] (1961)	2/3	2/3	$v^* = \sqrt{\rho_t v^2/H_B}$	H_B is Brinell hardness
4	Bruce [21] (1961)	1/2	2/3	$v^* = v/c_t$	
5	Eichelberger [106] (1962)	1/3	2/3	$v^* = \sqrt{\rho_t v^2/Y_t}$	
6	Loeffler et al. [107] (1963)	1/2	2/3	$v^* = v/c_t$	
7	Zhang and Huang [3] (2000)	0.448	0.563	$v^* = \sqrt{\rho_t v^2/Y_t}$	
8	Christman and Gehring [108] (1966)	2/3	2/3	$v^* = \sqrt{\rho_t v^2/Y_t}$	
9	Walsh and Johnson [109] (1964)	1/3	0.58	$v^* = v/c_t$	
10	Christiansen [110] (1993)	2/3	2/3	$v^* = v/c_t$	
11	Yu et al. [27] (1994)	0.725	2/3	$v^* = \sqrt{\rho_t v^2/Y_t}$	
12	Zhou et al. [111] (2000)	0.62	0.48	$v^* = \sqrt{\rho_t v^2/H_t}$	2.6 km/s < v < 5 km/s
		0.5	0.68		v > 5 km/s

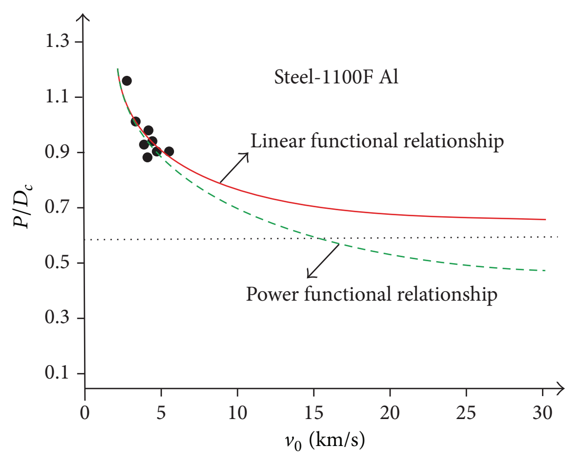

Figure 4: Comparison of the linear and power velocity models.

of higher velocity impact is semispherical, the conclusion that the linear function is more suitable to describe crater parameters than power function still needs to be confirmed further. Merzhievsky [38] established a predicted model considering the strain rate effect and gave the reason why the power of impact velocity is not equal to 2/3. He pointed out that the strength can affect the power and the kinetic energy would play a more important role than momentum. Additionally, the crater empirical formula for projectile hypervelocity impact on rock proposed by Gault [29] agreed with the 2/3 law. So it can be said that the 2/3 law can describe crater effect well.

3.3. Simple Theoretical Model for Crater. Because of the special characteristics of materials such as large deformation, multiphase, and nonlinearity, there are few of strictly theoretical models for crater parameters. Watts and Atkinson [39] pointed out that the plastic flow should be taken into account in crater radius analysis. With Bernoulli equation, Atkinson built a crater diameter calculation model for metal target under hypervelocity impact considering the dispersion effect:

$$\frac{D_c}{d_p} = \left(\frac{4}{3}\right)^{1/(N+1)} \left(\frac{\rho_p}{\rho_t}\right)^{1/(N+1)} \left(\frac{\rho_t}{Y_t}\right)^{1/(N+1)} \cdot \left(\frac{c_t}{c_p}\right)^{1/(N+1)} \left(\frac{v_0}{1+\sqrt{\rho_p/\rho_t}}\right)^{2/(N+1)}, \quad N > 2, \tag{11}$$

where $N > 2$ means the power of impact velocity is less than 2/3. The calculating method for crater depth was also obtained as

$$\frac{P}{d_p} = \begin{cases} \dfrac{1}{4}\left(\dfrac{4}{3}\right)^{1/3}\left(\dfrac{\rho_p}{\rho_t}\right)^{1/3}\left(\dfrac{\rho_t}{Y_t}\right)^{1/3} \cdot \left\{\left[c_0 + \dfrac{s_0\left(v_0 - v_{\mathrm{cnut}}\right)}{1+\sqrt{\rho_t/\rho_p}}\right]\left(v_0 - v_{\mathrm{cnut}}\right)\right\}^{1/3}, & v_0 < v_{\mathrm{crut}} = \dfrac{\sqrt{2\rho_t Y_t}}{1+\sqrt{\rho_t/\rho_p}}, \\ \dfrac{1}{4}\left(\dfrac{4}{3}\right)^{1/3}\left(\dfrac{\rho_p}{\rho_t}\right)^{1/3}\left(\dfrac{\rho_t}{Y_t}\right)^{1/3} \cdot \left(\dfrac{s_0}{1+\sqrt{\rho_t/\rho_p}}\right)^{1/3} v_0^{2/3}, & v_0 > v_{\mathrm{crut}} = \dfrac{\sqrt{2\rho_t Y_t}}{1+\sqrt{\rho_t/\rho_p}}, \end{cases} \tag{12}$$

where s_0 is the slope of the relationship curve between shock wave velocity and particle velocity. Equation (12) indicates that with impact velocity increase the power changes from 1/3 to 2/3 which agreed with the 2/3 law.

Zhou [40] established a projectile motion equation with the particle velocity and Bernoulli equation and obtained the calculating method for crater depth as

$$\frac{P}{d_p} = \frac{4\left(\rho_t c_t + \rho_p c_p\right)}{3a_p \rho_t c_p} \ln \frac{v_0}{\sqrt{Y_t/\rho_t}}, \tag{13}$$

where a_p is the shape coefficient of projectile. Based on the linear relationship between crater volume and projectile kinetic energy, the calculating method of crater radius was also established as

$$\frac{D_c}{d_p} = \left(\frac{\rho_p}{k_t \rho_t E_t}\right)^{1/3} v_0^{2/3}, \tag{14}$$

where E_t is the boiling energy of target and k_t is the amending coefficient with crush and kinetic energy of target considered. Equation (13) is just suitable for the penetration that the projectile is unbroken. Equation (14) has a certain physical base and considers the plastic flow; furthermore, k_t is defined as the parameter that is related to material crushing and kinetic energy.

Considering the similarity between impact crater and explosion crater and the impact pressure attenuation, Kadono and Fujiwara [41] established a crater depth calculation method for projectile ranges from unbroken to eroded by introducing a dimensionless coefficient ξ_t:

$$\frac{P}{d_p} = k_\xi \xi_t^{A_\xi} \left(\frac{\rho_p}{\rho_t}\right)^{B_\xi} \left(\frac{Y_p}{Y_t}\right)^{C_\xi} \ln f\left(v_0\right),$$
$$\xi_t = \begin{cases} \dfrac{\rho_t v_0^2}{Y_p}, & p_0 < Y_p, \\ \dfrac{p_0}{Y_p}, & p_0 > Y_p, \end{cases} \tag{15}$$

where $k_\xi \approx 1$, $A_\xi, B_\xi \approx 1$, and C_ξ are all constants and $f(v_0)$ is the function of impact velocity. This model reflects the effect of projectile states; however, some constants need to be obtained by experimental data fitting.

Though some parameters of the theories above depend on experimental results, they reveal some regularities of crater effect.

4. Theory of Long Rod Projectile Penetration into Semi-Infinite Target

Earth penetrator and armor piercing projectile are both long rod and have great penetration ability, so the researches on long rod penetration have received intensive attention. Experiments [42–53] show that with impact velocity increase long rod changes from rigid to deformed then to semifluid and to quasifluid state at last [54] as Figure 5 shows. So it is necessary to build a multistage engineering calculation model including different projectile states. Quasifluid projectile penetration can be solved with Bernoulli equation [55–57]. The crater depth is not related to the impact velocity but projectile length L_p and $L_p\sqrt{\rho_p/\rho_t}$ (where ρ_p and ρ_t are the densities of

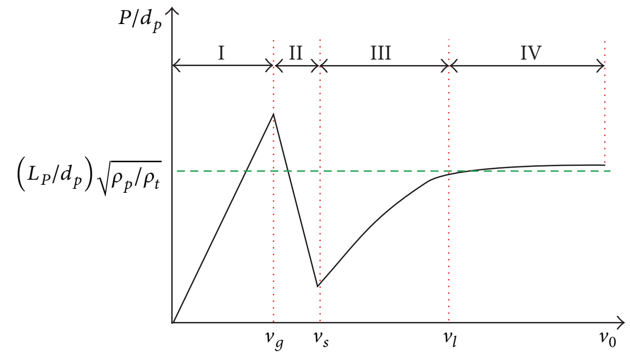

Figure 5: Dimensionless penetration depth versus projectile impact velocity.

projectile and target, resp.). For rigid projectile penetration, satisfying results can be obtained with cavity-expansion theory [58–62] and internal friction theory [63–69]. In the internal friction theory, the higher stress and the rapid velocity change occur only in a certain narrow zone; the stress wave is almost identical to a shock wave and exhibits "short wave" properties. Therefore, in the plastic region, the material's compressibility is considered with the sound speed. In the cracked region, the unstable propagation and spontaneous growth of crack were used to get the boundary conditions. The researches on determining projectile state, the engineering calculation models for semifluid projectile, and deformed projectile penetration are reviewed below.

4.1. Division of Projectile Penetration States. From Figure 5, it can be seen that the upper limit v_l and lower limit v_s of semifluid projectile penetration and the lower limit v_g of deformed projectile are three critical points for dividing penetration states. As the impact velocity increases, the final depth of penetration approaches a hydrodynamic limit in the quasifluid regime. Semifluid and quasifluid states are both obtained with Bernoulli equation. When the impact velocity reaches a certain value, the effect of strength is very small. Additionally, most of the impact velocities of earth penetrators and armor piercing projectiles are within semifluid state range [54, 70], so v_s and v_g are the key points for dividing projectile penetration states.

Based on Forrestal's cavity-expansion theory [71], Li and Chen proposed a dimensionless calculating method for rigid projectile penetration depth [62]; the determining method for v_g was deduced as follows [70]:

$$I_r = \frac{m_p v_g^2}{A_t N_1 d_p^3 \sigma_t}, \tag{16a}$$

$$I_r = N\left(6.1896 \cdot I_r^{-0.3094} \frac{\sigma_p}{\sigma_t A_t} - 1\right), \tag{16b}$$

where I_r is the dimensionless parameter obtained by experimental data fitting, A_t is the dimensionless parameter of target, N_1 is the dimensionless warhead shape parameter, m_p is the projectile mass, σ_t is the target material strength, and N is the dimensionless projectile shape parameter.

Based on the experimental results of concrete, Mu [72] used the moment that warhead appears semisphere as the up limit of rigid projectile penetration; according to the relationship between mass loss rate of projectile and initial impact kinetic energy, v_s was obtained as

$$v_g = \left[\frac{2(\gamma_{0.5} - K_g)}{C_g} \right]^{0.5}, \tag{17}$$

where C_g and K_g are both empirical constants and $\gamma_{0.5}$ is the mass proportion of spherical warhead to whole projectile.

According to Segletes's [73] view that the projectile was constrained by target in initial penetration phase and the erosion is difficult to occur, Lou [74] used the Bishop et al. [75] and Hill's [76] critical pressure P_c of crater for the compressible materials and Rosenberg's relation $P_c \approx 3Y_t$ [77, 78] obtained:

$$v_g = \sqrt{\frac{2Y_p + 3Y_t - R_t}{\rho_t}}. \tag{18}$$

The determining methods for v_g proposed by Chen, Li, and Mu all need experimental data fitting. The method presented by Lou does not depend on experiments; however, there are great differences between the predicted results and experiments. Calculations show that these methods can only give rough ranges, so it is necessary to research more accurate ones with physical and mechanical bases.

The determining method for the lower limit v_s of semifluid projectile was proposed by Tate [57] who presented the critical velocities for different projectile-target groups as

$$v_s = \begin{cases} \sqrt{\dfrac{2(R_t - Y_p)}{\rho_p}}, & R_t > Y_p, \\ \sqrt{\dfrac{2(Y_p - R_t)}{\rho_p}}, & R_t < Y_p. \end{cases} \tag{19}$$

In 1977, Tate [79] deemed that the lower limit v_s is related to the erosion rate and propagation of plastic wave, and if the former is greater than the latter, the projectile would enter into semifluid state, and obtained

$$v_s = \begin{cases} \sqrt{\dfrac{E_{ap}}{\rho_p}} \left\{ 1 + \sqrt{\dfrac{\rho_p}{\rho_t} \left[1 - \dfrac{2(R_t - Y_p)}{E_{ap}} \right]}, \right. & R_t < Y_p, \\ \sqrt{\dfrac{E_{ap}}{\rho_p}}, & R_t > Y_p, \end{cases} \tag{20}$$

where E_{ap} is the shear modulus of projectile material. Calculations manifested that the results of (19) are closer to experiments than (20) and could evaluate the states of deformed and semifluid projectiles well.

4.2. Engineering Calculating Model for Semifluid Projectile. For semifluid projectile penetration, mere portion of projectile is quasifluid. Therefore, the strength of projectile and target could not be neglected. Alekseevskii [80] and Tate [57] established the famous modified Bernoulli equation successively with projectile erosion considered:

$$\frac{1}{2}\rho_p (v - u)^2 + Y_p = \frac{1}{2}\rho_t u^2 + R_t. \tag{21}$$

Equation (21) was applied widely and researched deeply on how to determine the strength team of projectile and target and how to consider the effect of mushroom head.

Alekseevskii [80] used dynamic hardness H_t of target as the strength team and obtained

$$\frac{1}{2}\rho_p (v - u)^2 + Y_p = \frac{1}{2}\rho_t u^2 + H_t. \tag{22}$$

H_t has explicit physical mean that is plastic work of unit material deforming and has been used by researchers in former Soviet Union to describe material strength. Zlatin and Vitman's book proposed the testing methods for dynamic hardness and also pointed out that it reflects the deformed obstruction of material under local extrusion of dynamic loading [81–84].

Tate suggested Y_p is equal to elastic limit value $Y_{p\text{-HEL}}$ [57]:

$$Y_p = Y_{p\text{-HEL}} = \frac{1 - \upsilon}{1 - 2\upsilon} \sigma_{yp}, \tag{23}$$

where υ is the Poisson ratio and σ_{yp} is the yield strength under uniaxial stress. The physical mean of R_t is not clear and depends on elastic-plastic analysis. Tate gave new forms of Y_p and R_t with the fitting results from experimental data [85, 86]:

$$Y_p = 1.7\sigma_{yp}, \qquad R_t = \sigma_{yt} \left[\frac{2}{3} + \ln\left(\frac{2E_t}{3\sigma_{yt}} \right) \right], \tag{24}$$

where σ_{yt} is the dynamic yield strength of target and E_t is Young modulus of target. It can be seen that Tate modified the model by changing strength term of target and also illustrated the complexity of target strength determination.

Sun et al. [87] supposed that both the inertia and the strength of target affect the penetration. They took the difference between cross-sectional area and pressure area of crater bottom into account and proposed a modified calculating model for long rod:

$$\begin{aligned} &2\rho_p (v - u)^2 + \sigma_{yp} \\ &\quad = 3\rho_t u^2 + \frac{4}{3}\sigma_{yt} \left[1 + \ln\left(\frac{2E_t}{3\sigma_{yt}} \right) \right] + \frac{4}{27}\pi^2 E_h, \end{aligned} \tag{25}$$

where E_h is the enhanced elastic modulus of target material.

Considering the inhomogeneity of the force distributing from mushroom head to centerline of long rod during penetration, Rosenberg et al. [88] obtained a modified Bernoulli equation by introducing the equivalent area as

$$\begin{aligned} & 2\rho_p (v-u)^2 + \frac{1-\upsilon}{1-2\upsilon}\sigma_{yp} \\ & \quad = \rho_t u^2 + \frac{2\sigma_{yt}}{\sqrt{3}}\left[1+\ln\frac{2E_t}{(5-4\upsilon)\,\sigma_{yt}}\right]. \end{aligned} \tag{26}$$

Zhang and Huang [89] regarded the warhead of long rod as hemisphere during the penetrating progress and obtained the A-T model by using Rosenberg's method. The strength steam of projectile and target could be expressed as

$$\begin{aligned} & \frac{1}{2}\rho_p (v-u)^2 + \frac{1-\upsilon}{4(1-2\upsilon)}\sigma_{yp} \\ & \quad = \frac{3}{4}\rho_t u^2 + \frac{2\sigma_{yt}}{3}\left[1+\ln\frac{2E_t}{3\sigma_{yt}}\right]. \end{aligned} \tag{27}$$

The derivation of (25), (26), and (27) has same two main points. Firstly, the view that the cross-sectional area of mushroom head is two times the warhead's was adopted. Secondly, the target strength was determined with cavity-expansion theory.

Based on numerical calculation results, Anderson et al. [90] deduced the deformed range of projectile and obtained the relationship between resistance and penetrating velocity with the cylindrical cavity-expansion theory and established a modified Bernoulli equation as

$$\frac{1}{2}\rho_p (v-u)^2 + \sigma_{yp} = \frac{1}{2}\rho_t u^2 + \frac{7}{3}\ln a_k \sigma_{yt}, \tag{28a}$$

$$\left(1+\frac{\rho_t u^2}{\sigma_{yt}}\right)\sqrt{K_t - \rho_t a_k^2 u^2} = \left(1+\frac{\rho_t a_k^2 u^2}{2G_t}\right)\sqrt{K_t - \rho_t u^2}. \tag{28b}$$

Wen and Lan [90–92] divided the original plastic zone into fluid zone and plastic zone (Figure 6). They supposed that if impact velocity is greater than the critical velocity U_{F0}, the quasifluid part thickness in target material would keep invariant. Hence, a modified Bernoulli equation was obtained as

$$\begin{aligned} & \frac{1}{2}\rho_p (v_0-u)^2 + \frac{1-\upsilon}{1-2\upsilon}\sigma_{yp} \\ & \quad = \frac{1}{2}\rho_t u^2 + S_F + 2\rho_t U_{F0}^2 \exp\left[-2\left(\frac{u-U_{F0}}{nU_{F0}}\right)^2\right] \\ & \quad\quad - \rho_t u U_{F0} \exp\left[-\left(\frac{u-U_{F0}}{nU_{F0}}\right)^2\right], \end{aligned} \tag{29}$$

where S_F is the static resistance and U_{F0} is the critical velocity, $n \approx 2.45$.

Equations (28a), (28b), and (29) take the effect of impact velocity into account. Tate [57] pointed out that strength R_t may change with penetration depth and velocity, so the strength terms in (28a), (28b), and (29) are closer to the penetration process than other models. The measurement of dynamic hardness in Alekseevskii's model has taken the effect of impact velocity into account. Kozhushko et al. [93] also proposed a strength determining method considering the effect of impact velocity as

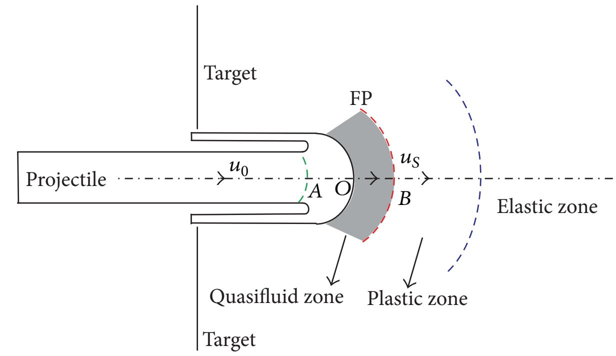

Figure 6: Response regions along the centerline in the target under high impact velocity.

$$R_t = 0.5u^2\left[\rho_t - \rho_p\left(\frac{v}{u}-1\right)^2\right]. \tag{30}$$

Above all, target material strength and the difference between cross-sectional area of projectile and area of bottom are two key factors in engineering calculating model for semi-fluid projectile, and which are all neglected in models above. It is necessary to establish a new calculating model considering the integrated effects.

4.3. Engineering Calculation Models for Deformed Projectile.

From the experiments of metal [42, 43], dry sand [44, 45], rock [46], and concrete [47–55], it can be found that with impact velocity increase projectile can sustain obvious erosion, blunting, even bending, and crushing, and penetration depth decreases greatly. Projectile deformation is closely related to the design and optimization for high-velocity/hypervelocity weapon. Penetration mechanism of deformed projectile has been a hot topic at present. He et al. [54] summarized the research progress of projectile erosion effect for projectile penetrating into concrete and mainly analyzed the physical progress of projectile erosion and mass loss and pointed out that the projectile erosion research under the coupling effect of melting and shearing needs to be developed further. Because of the above, the engineering calculating models for deformed projectile are focused on here.

Zhao et al. [94] pointed out that with initial impact velocity increase warhead changes from ogival to semispherical and even more blunt. According to the linear relationship between initial impact velocity v_0 and the shape coefficient of remaining warhead N_r^*, the relationship between shape coefficient of warhead N^* and instantaneous penetration velocity u was established as

$$N^* = N_r^* - k_r u^2 = N_i^* + k_r\left(v_0^2 - u^2\right), \tag{31}$$

where k_r is a fitting parameter and N_i^* is the shape coefficient of initial warhead. According to the calculating method proposed by Li and Chen [62], the current projectile mass during penetrating was given by using the Silling and Forrestal empirical formula [95]:

$$m_r = m_p - \frac{1}{2} m_p C_r \left(v_0^2 - u^2 \right), \tag{32}$$

where m_r is the projectile current mass, m_p is the projectile initial mass, and C_r is the fitting coefficient.

Supposing that the projectile mass and warhead shape keep invariant within a time during penetration, a penetration calculating model for deformed projectile can be obtained from (31) and (32) and Forrestal et al.'s [71] rigid projectile penetration calculation method. Though this model is a semiempirical formula, it is realizable and can be used in calculation.

Zhao [51] supposed that the relationship between warhead mass loss and velocity is fully quadratic polynomial; the warhead shape would change from ogival to semispherical, then to obtuse and flat with impact velocity increases. The relationship between residual projectile mass and shape was obtained as

$$m_r = \pi \rho_p r_p^2 \left(k_f r_p + L \right), \tag{33}$$

where r_p is the projectile radium, k_f is the warhead length converting coefficient of residual projectile, and L is the projectile original length. Zhao wrote a program for calculating penetration depth whose results are in good agreement with experiment data for low impact velocity; however, there are great differences between them when velocity is above 1200 m/s.

He [96, 97] found that the effect on penetration depth is not the mass loss but the warhead shape. According to Jones's [98] expression of projectile mass loss, by introducing a correction coefficient to describe the effect that material shedding and target material hardness on projectile mass loss, He [97, 99] gave the expression of mass increment:

$$dm = \frac{-\eta \varsigma \pi d_p^2 \tau_0 N_1^* m u}{4\kappa Q F_n + \eta \varsigma \pi d_p^2 \tau_0 N_1^* u^2} du, \tag{34}$$

where η is the correction coefficient, ς is the coefficient related to the projectile shape, τ_0 is the shear strength of target material, κQ is the melting heat of unit mass projectile, F_n is the force on projectile, N_1^* is the projectile shape coefficient, and u is the penetration velocity. Warhead shape keeps invariant within every calculating time step, and after that shape can be determined from the increment of warhead mass. The increment of penetration depth is obtained as

$$dp = \frac{u_{i-1}^2 \Delta m_i + m_{i-1} u_{i-1}}{F_{n,i-1}} du. \tag{35}$$

He's model can predict not only projectile mass loss and nose shape blunting but also penetration depth, time histories of projectile velocity, and accelerated velocity. Additionally, He [97] also established a model for describing friction work rate within unit area of projectile. He extended Jones's model to predict local projectile mass loss and built another numerical calculating model for simulating projectile mass loss and nose shape blunting. The cavity-expansion theory was used to describe surface pressure of projectile in the two models; however, the projectile surface backing because of mass loss could affect surface pressure. Additionally, the target material may have entered into quasifluid state and different models to describe surface pressure are needed.

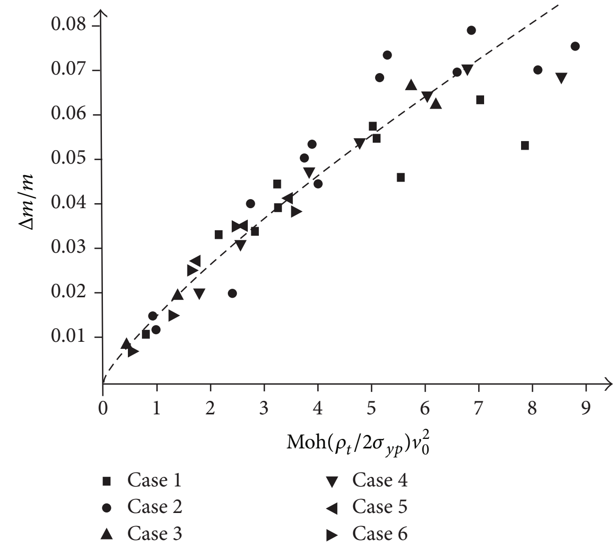

Figure 7: The power relationship between mass erosion and modified dimensionless initial kinetic energy.

Yang [100] deduced the dimensionless equation of mass loss for projectile penetration into concrete:

$$\frac{\Delta m}{m} = a_0 \left(\mathrm{Moh} \frac{\rho_t}{2\sigma_{yp}} v_0^2 \right)^{b_0}, \tag{36}$$

where a_0 and b_0 are the dimensionless parameters obtained by experimental data fitting as shown in Figure 7. Moh is the Mohs hardness of target. From (36), the projectile erosion speed can be expressed as

$$v_a = \frac{2 a_0 b_0}{\rho_p} \left(\mathrm{Moh} \frac{\rho_t}{2\sigma_{yp}} v_0^2 \right)^{b_0} u^{2b_0 - 1} F_n \left(\sin\theta + \mu_f \cos\theta \right), \tag{37}$$

where μ_f is the friction coefficient and θ is the intersection angle of tangential direction and axial direction of warhead. Using (36) and (37), Yang constructed a set of difference equations in which the results indicated that erosion has little influence on penetrating depth.

Wen and Lan [101] supposed that the change of warhead just happens at the moment of impact and then keeps spherical and cross-sectional area keeps A_d. As shown in Figure 8, the velocities of particles in deformed zones are all u_s. There are jumps for particle velocity and cross-sectional area in surface EP and the pressure in EP is uniformity, and the crater

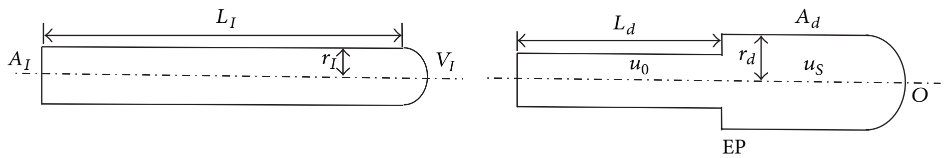

FIGURE 8: The deformed projectile.

area keeps invariant. The relationship between velocity of projectile tail and penetration velocity can be obtained as

$$u_0 = \sqrt{\frac{f(u_s)(A_d/A_I - 1) - Y_p(1 - A_I/A_d)}{\rho_p}} + u_s, \quad (38)$$

where u_s is the penetration velocity and $f(u_s) = 2\pi r_d^2 \int_0^{\pi/2} \sigma(\theta) d\theta$ is the force on unit area of warhead after deformation. Based on the results of experiments and numerical simulations, the following equation is yielded

$$\frac{A_d}{A_I} = a_u \left(\frac{V_I}{V_g} - 1 \right)^2 + 1, \quad (39)$$

where a_u is determined by experiments. The calculating equation of penetration depth for deformed projectile was obtained as

$$P_D = \frac{\rho_p L_I}{Y_p} \cdot \int_{V_S}^{V_I} u_s \exp \left[\frac{A_d \rho_p}{(A_d - A_I) Y_p} \int_{V_i}^{u_0} (u_0 - u_s) \, du_0 \right] du_0. \quad (40)$$

Rosenberg and Dekel indicated that the deformation of warhead takes place within a short time in the initial phase of impact [78] as Figure 9 shows. With Rosenberg's view, Lou [74] considered that the instantaneous deformation leads to the cross-sectional area increases and then projectile keeps steady. According to the results of Forrestal and Warren [102] and Rosenberg and Dekel [78], Lou modified the target resistance on indeformable long rod projectile by multiplying a cross-sectional coefficient K_s (see Figure 10) and obtained a calculation equation of deformed projectile penetration depth with Forrestal's model:

$$\frac{P}{L_{\text{eff}}} = \frac{1}{3N} \left(\frac{\rho_p}{\rho_t} \right) \ln \left(1 + \frac{3N \rho_t v_0^2}{2 K_s R_t} \right). \quad (41)$$

Equations (40) and (41) both take the warhead blunting into account. Equation (40) considers the change of projectile during the blunting progress while (41) does not. At the same time, it can be seen that there is no conclusion on the effect of projectile mass erosion. The effect of warhead blunting and erosion on penetration still needs to be studied more clearly and the blunting degree prediction of warhead depends on experiments greatly.

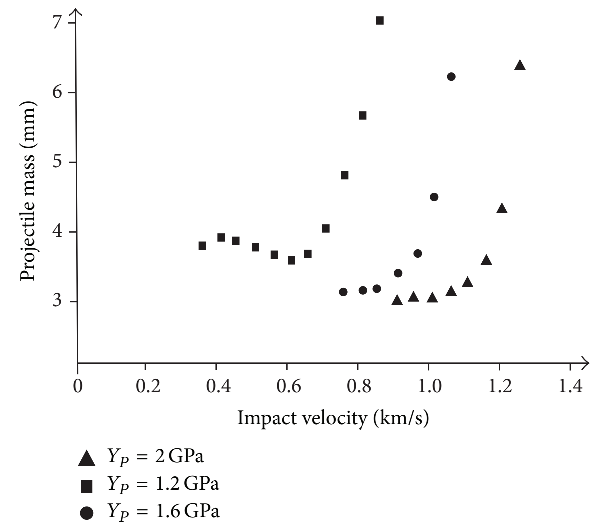

FIGURE 9: Numerical calculating results of Rosenberg and Dekel [78].

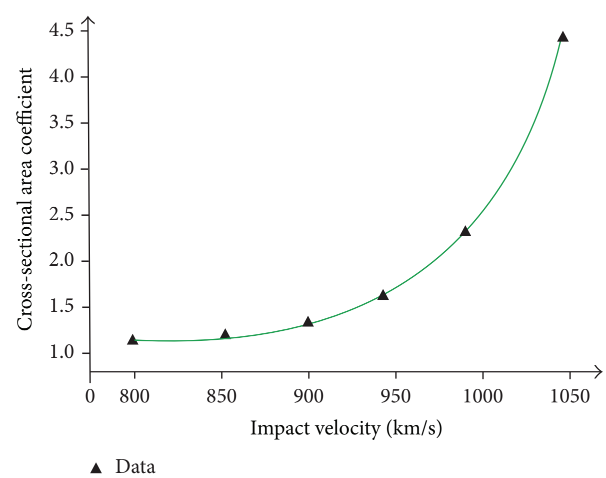

FIGURE 10: The relationship between K_s and impact velocity.

5. Conclusions

Through many decades of research, the preliminary evaluation of velocity for projectile high-velocity/hypervelocity impact on semi-infinite target, crater effect of spherical projectile, and penetration depth calculating model for long rod projectile have been established; however, there are some problems which need to be solved further.

(1) The situations that the strength could be neglected and the compressibility takes leading position can be seen as the conditions for high-velocity and hypervelocity impact. However, a more accurate method for determining the critical value of high-velocity impact is needed.

(2) The semispherical crater shape is not suitable for all conditions in hypervelocity impact by spherical projectiles. The crater shapes of metal targets for impact velocity above 8 km/s and geologic material target in hypervelocity impact need to be ascertained. The empirical formulae and theoretical models for geologic materials cannot meet the practical needs and should be studied further.

(3) For long rod projectile penetrating into semi-infinite target, the current evaluation methods for upper limit of rigid projectile state can just give rough ranges and there is a need to establish a multiphase calculation model including all states.

(4) The target material strength and the difference between projectile sectional area and pressure area of crater bottom influenced by penetration velocity are two key factors for semifluid projectile penetration. The engineering calculating model considering the effect of them for semifluid projectile is needed to be established.

(5) It is necessary to establish a new engineering calculating model which is more suitable to penetration physical and mechanical characteristics for deformed projectile.

Conflict of Interests

The authors declare that there is no conflict of interests regarding the publication of this paper.

Acknowledgments

The authors gratefully acknowledge the financial supports from Program for Changjiang Scholars and Innovative Research Team in University (no. IRT13071), the Science Fund for Creative Research Group of the National Natural Science Foundation of China (Grant 510210001), projects supported by the National Natural Science Foundation of China (Grants 51409258, 51309233, and 51378498), and project supported by State Key Laboratory for Disaster Prevention & Mitigation of Explosion & Impact Foundation (Grant DPMEIKF201301).

References

[1] R. Kinslow, *High-Velocity Impact Phenomena*, Academic Press, New York, NY, USA, 1970.

[2] W. Herrmann and J. S. Wilbeck, "Review of hypervelocity penetration theories," *International Journal of Impact Engineering*, vol. 5, no. 1–4, pp. 307–322, 1987.

[3] Q.-M. Zhang and F. L. Huang, *Hypervelocity Impact Kinetics Theory. First Version*, Science Press, Beijing, China, 2000, (Chinese).

[4] T. H. Antoun, L. A. Glenn, O. R. Walton, P. Goldstein, I. N. Lomov, and B. Liu, "Simulation of hypervelocity penetration in limestone," *International Journal of Impact Engineering*, vol. 33, no. 1–12, pp. 45–52, 2006.

[5] V. M. Fomin, A. I. Gulidov, G. A. Salozhnikov et al., *The High-Speed Interaction between Solids*, The Russian Academy of Science Siberian Branch Press, Novosibirsk, Russia, 1999, (Russian).

[6] T. J. Ahrens and M. L. Johnson, "Shock wave data for rocks," in *Mineral Physics and Crystallography, A Handbook of Physical Constants*, T. J. Ahrens, Ed., pp. 35–44, American Geophysical Union, Washington, DC, USA, 1995.

[7] G. Weirauch, *Das verhalfen von kupfersufen derm auftreffen auf verschiedene werkstuffe mit geschwindigkeiten zwischen 50m/s and 1650m/s*, University of Karlsruhe, Karlsruhe, Germany, 1971.

[8] F.-Q. Jing, *Experiment State Equation Guiding. Second Version*, Science Press, Beijing, China, 1999, (Chinese).

[9] W. P. Walters and J. A. Zukas, *Theory and Application of Shaped Charge*, Weapon industry Press, Beijing, China, 1989, Translated 1992 by W. Shu-kui and B. Jing-fen.

[10] J. D. Walker, "Hypervelocity penetration modeling: momentum vs. energy and energy transfer mechanisms," *International Journal of Impact Engineering*, vol. 26, no. 1–10, pp. 809–822, 2001.

[11] Q.-H. Qian and M.-Y. Wang, *Shock and Explosion Effect in Rock*, First Version, National Defense Industry Press, Beijing, China, 2010 (Chinese).

[12] G. H. Jonas and J. A. Zukas, "Mechanics of penetration: analysis and experiment," *International Journal of Engineering Science*, vol. 16, no. 11, pp. 879–903, 1978.

[13] F.-Q. Jing, "Hypervelocity impact phenomena," *Explosion and Shock Waves*, vol. 10, pp. 279–288, 1990 (Chinese).

[14] M.-Y. Wang, *Calculating Research Progress on Protective Structure Anti-Penetration*, Xiangshan Science Conferences Reports, Beijing, China, 2013, (Chinese).

[15] J. L. Summers and A. C. Charters, "High speed impact of metal projectiles in targets of various materials," in *Proceedings of the 3rd Symposium on Hypervelocity Impact*, Chicago, Ill, USA, October 1958.

[16] A. C. Charters and G. S. Locke Jr., "A preliminary investigation of high speed impact: the penetration of small spheres into thick copper targets," Tech. Rep. NASA RM A58B26, 1957.

[17] J. Frazier, "Hypervelocity impact experiments in wax," BRL Report 1124, Aberdeen Proving Ground, Aberdeen, Md, USA, 1961.

[18] J. H. Kineke Jr., "An experimental study of crater formation in metallic targets," in *Proceedings of the 4th Symposium on Hypervelocity Impact*, vol. 1, pp. 10–12, 1960.

[19] J. H. Kineke Jr., "Observation of crater formation in ductuile materials," in *Proceedings of the 5th Symposium on Hypervelocity Impact*, pp. 339–370, Denver, Colo, USA, October 1961.

[20] W. Herrmann and A. Jones, "Correlation of hypervelocity impact data," in *Proceedings of the 5th Symposium on Hypervelocity Impact*, pp. 389–438, Denver, Colo, USA, 1961.

[21] E. P. Bruce, "Review and analysis of high velocity impact data," in *Proceedings of the 5th Symposium on Hypervelocity Impact*, pp. 439–474, Denver, Colo, USA, 1961.

[22] G.-C. Sun, Q.-M. Tan, C.-X. Zhao, and X.-Z. Ge, "Cratering experiments with hypervelocity impact upon thick metallic targets," *Acta Armamentarii*, vol. 1, pp. 27–31, 1994 (Chinese).

[23] K. P. Stanyukovich, *The Unsteady Motion of Continuum*, Nauka, Moscow, Russia, 1971.

[24] L. V. Leontyev, "Comparison for effects of meteoroid collision with the surfaces of different targets," *Space Research*, vol. 14, pp. 278–286, 1976.

[25] L. E. Murr, S. A. Quinones, E. Ferreyra T et al., "The low-velocity-to-hypervelocity penetration transition for impact craters in metal targets," *Materials Science and Engineering A*, vol. 256, no. 1-2, pp. 166–182, 1998.

[26] J. R. Baker, "Hypervelocity crater penetration depth and diameter—a linear function of impact velocity?" *International Journal of Impact Engineering*, vol. 17, no. 1–3, pp. 25–35, 1995.

[27] S.-B. Yu, G.-C. Sun, and Q.-M. Tan, "Experimental laws of cratering for hypervelocity impacts of spherical projectiles into thick target," *International Journal of Impact Engineering*, vol. 15, no. 1, pp. 67–77, 1994.

[28] E. J. Öpik, "The moon's surface," *Annual Review of Astronomy and Astrophysics*, vol. 7, pp. 473–526, 1969.

[29] D. E. Gault, "Displaced mass, depth, diameter, and effects of oblique trajectories for impact craters formed in dense crystalline rocks," *The Moon*, vol. 6, no. 1-2, pp. 32–44, 1973.

[30] M. R. Dence, R. A. F. Grieve, and P. B. Robertson, "Terrestrial impact structures: principal characteristics and energy consideration," in *Impact and Explosion Cratering*, D. J. Roddy, R. O. Pepin, and R. B. Merrill, Eds., pp. 247–275, Pergamon Press, New York, NY, USA, 1977.

[31] Q.-M. Zhang and F.-L. Huang, "Effects on the earth resulted from the impact of a planetoid," *China Safety Science Journal*, vol. 5, pp. 21–26, 1995.

[32] P. S. Westine and S. A. Mullin, "Scale modeling of hypervelocity impact," *International Journal of Impact Engineering*, vol. 5, no. 1–4, pp. 693–701, 1987.

[33] Y.-M. Shen and J.-Q. Chen, "Numerically simulating verification of the comparability rule on hypervelocity impact," *Explosion and Shock Waves*, vol. 31, no. 4, pp. 343–348, 2011 (Chinese).

[34] R. T. Sedgwick, "Numerical techniques for modeling high velocity penetration and perforation processes," in *Ballistic Materials and Penetration Mechanics*, R. C. Laible, Ed., vol. 5, pp. 253–272, Elsevier, New York, NY, USA, 1980.

[35] J.-L. Xiang, *The Effect of Compressible Effect of Metal Materials to Crater of Hypervelocity Impacting into Secondary Targets*, Mechanics Research Institution of Chinese Academy of Sciences, Beijing, China, 1990, (Chinese).

[36] Z.-W. Luo, *Numerical Simulation of Metal Material Hypervelocity Impact*, Mechanics Research Institution of Chinese Academy of Sciences, Beijing, China, 1990, (Chinese).

[37] Q. Guo, *The Hypervelocity Impact Activity of TC4 Fibre and TiB2 Grains Enhanced Aluminum-Based Composite Material*, Harbin Institute of Technology, Harbin, China, 2012.

[38] L. A. Merzhievsky, "Crater formation in a plastic target under hypervelocity impact," *International Journal of Impact Engineering*, vol. 20, no. 6-10, pp. 557–568, 1997.

[39] A. J. Watts and D. Atkinson, "Dimensional scaling for impact cratering and perforation," Tech. Rep. NASA-CR-188259, NASA, Washington, DC, USA, 1995.

[40] N. Zhou, "A simple analysis model for the hypervelocity cratering of semi-infinite targets by projectile," *International Journal of Impact Engineering*, vol. 23, no. 1, pp. 989–994, 1999.

[41] T. Kadono and A. Fujiwara, "Cavity and crater depth in hypervelocity impact," *International Journal of Impact Engineering*, vol. 31, no. 10, pp. 1309–1317, 2005.

[42] A. J. Piekutowski, M. J. Forrestal, K. L. Poormon, and T. L. Warren, "Penetration of 6061-T6511 aluminum targets by ogive-nose steel projectiles with striking velocities between 0.5 and 3.0 KM/S," *International Journal of Impact Engineering*, vol. 23, no. 1, pp. 723–734, 1999.

[43] M. J. Forrestal and A. J. Piekutowski, "Penetration experiments with 6061-T6511 aluminum targets and spherical-nose steel projectiles at striking velocities between 0.5 and 3.0 km/s," *International Journal of Impact Engineering*, vol. 24, no. 1, pp. 57–67, 2000.

[44] A. F. Savvateev, A. V. Budin, V. A. Kolikov, and P. G. Rutberg, "High-speed penetration into sand," *International Journal of Impact Engineering*, vol. 26, no. 1-10, pp. 675–681, 2001.

[45] S. J. Bless, D. T. Berry, B. Pedersen et al., "Sand penetration by highspeed projectiles," in *Shock Compression of Condensed Matter*, M. L. Elert, W. T. Buttler, M. D. Furnish, and etal, Eds., pp. 1361–1364, American Institute of Physics, 2009.

[46] J. Shen, X. Xu, X. He, S. Feng, and J. Yang, "Experimental study of effect of rock targets penetrated by high-velocity projectiles," *Chinese Journal of Rock Mechanics and Engineering*, vol. 29, no. 2, pp. 4207–4212, 2010 (Chinese).

[47] M. J. Forrestal, D. J. Frew, S. J. Hanchak, and N. S. Brar, "Penetration of grout and concrete targets with ogive-nose steel projectiles," *International Journal of Impact Engineering*, vol. 18, no. 5, pp. 465–476, 1996.

[48] D. J. Frew, S. J. Hanchak, M. L. Green, and M. J. Forrestal, "Penetration of concrete targets with ogive-nose steel rods," *International Journal of Impact Engineering*, vol. 21, no. 6, pp. 489–497, 1998.

[49] X.-W. Chen, B. Liang, Y.-Q. Ji et al., "Secondary-caliber experimental research on advanced high penetration ability earth penetrator," in *Proceedings of the Assembly Documents of the 6th National Conference on Security and Protective of Engineering Structure*, pp. 1–6, Luoyang, China, 2007, (Chinese).

[50] X. He, X.-Y. Xu, G.-J. Sun, J. Shen, J.-C. Yang, and D.-L. Jin, "Experimental investigation on projectiles' high-velocity penetration into concrete targets," *Explosion and Shock Waves*, vol. 30, no. 1, pp. 1–6, 2010 (Chinese).

[51] X.-N. Zhao, *Effect Research on High Velocity Projectile Penetrating into Concrete*, Nanjing University of Science and Technology, Nanjing, China, 2011, (Chinese).

[52] Z. Mu and W. Zhang, "An investigation on mass loss of ogival projectiles penetrating concrete targets," *International Journal of Impact Engineering*, vol. 38, no. 8-9, pp. 770–778, 2011.

[53] H.-J. Wu, F.-L. Huang, Y.-N. Wang, Z.-P. Duan, and A.-G. Pi, "Experimental investigation on projectile nose eroding effect of high-velocity penetration into concrete," *Acta Armamentarii*, vol. 33, no. 1, pp. 48–55, 2012 (Chinese).

[54] L.-L. He, X.-W. Chen, and Y.-M. Xia, "A review on the mass loss of projectile," *Acta Armamentarii*, vol. 31, no. 7, pp. 950–966, 2010 (Chinese).

[55] M. A. Lavrent'ev, "Cumulative charge and the principles of its operation," *Uspekhi Matematicheskikh Nauk*, vol. 12, no. 4, article 76, pp. 41–56, 1957.

[56] F. F. Vitman and N. A. Zlatin, "On collision of deformable bodies and its modeling," *Journal of Technology Physics*, vol. 33, pp. 982–989, 1963 (Russian).

[57] A. Tate, "A theory for the deceleration of long rods after impact," *Journal of the Mechanics and Physics of Solids*, vol. 15, no. 6, pp. 387–399, 1967.

[58] S. Satapathy, "Dynamic spherical cavity expansion in brittle ceramics," *International Journal of Solids and Structures*, vol. 38, no. 32-33, pp. 5833–5845, 2001.

[59] M. J. Forrestal, K. Okajima, and V. K. Luk, "Penetration of 6061-T651 aluminum targets with rigid long rods," *Journal of Applied Mechanics, Transactions ASME*, vol. 55, no. 4, pp. 755–760, 1988.

[60] S. C. Hunter and R. J. M. Crozier, "Similarity solution for the rapid uniform expansion of a spherical cavity in a compressible elastic-plastic solid," *The Quarterly Journal of Mechanics and Applied Mathematics*, vol. 21, no. 4, pp. 467–486, 1968.

[61] X. W. Chen and Q. M. Li, "Deep penetration of a non-deformable projectile with different geometrical characteristics," *International Journal of Impact Engineering*, vol. 27, no. 6, pp. 619–637, 2002.

[62] Q. M. Li and X. W. Chen, "Dimensionless formulae for penetration depth of concrete target impacted by a non-deformable projectile," *International Journal of Impact Engineering*, vol. 28, no. 1, pp. 93–116, 2003.

[63] M.-Y. Wang, X.-L. Rong, Q.-H. Qian, and T. Ge, "Calculation principle for penetration and perforation of projectiles into rock," *Chinese Journal of Rock Mechanics and Engineering*, vol. 22, no. 11, pp. 1811–1806, 2003.

[64] M.-Y. Wang, D.-L. Zheng, and Q.-H. Qian, "Scaling problems of penetration and perforation for projectile into concrete media," *Explosion and Shock Waves*, vol. 24, no. 2, pp. 108–114, 2004 (Chinese).

[65] W. Chen, M.-Y. Wang, and L.-Y. Gu, "Calculation of oblique penetration depth of projectiles into an intrinsic friction medium," *Explosion and Shock Waves*, vol. 28, no. 6, pp. 521–526, 2008 (Chinese).

[66] Q.-H. Qian and M.-Y. Wang, *Calculation Theory for Advanced Protective Structures*, first version, Jiangsu Science and Technology Press, Nanjing, China, 2009, (Chinese).

[67] M.-Y. Wang, T. Ge, P. Wu, and Q.-H. Qian, "Study on problems of near cavity of penetration and explosion in rock," *Chinese Journal of Rock Mechanics and Engineering*, vol. 23, pp. 2859–2863, 2005 (Chinese).

[68] D.-R. Wang, T. Ge, Z.-P. Zhou, and M.-Y. Wang, "Investigation of calculation method for anti-penetration of reactive power steel fiber concrete (RPC)," *Explosion and Shock Waves*, vol. 26, no. 4, pp. 367–372, 2006 (Chinese).

[69] M.-Y. Wang, K.-K. Tan, H.-J. Wu, and Q. Qian, "New method of calculation of projectile penetration into rock," *Chinese Journal of Rock Mechanics and Engineering*, vol. 28, no. 9, pp. 1863–1869, 2009 (Chinese).

[70] X. W. Chen and Q. M. Li, "Transition from nondeformable projectile penetration to semihydrodynamic penetration," *Journal of Engineering Mechanics*, vol. 130, no. 1, pp. 123–127, 2004.

[71] M. J. Forrestal, B. S. Altman, J. D. Cargile, and S. J. Hanchak, "An empirical equation for penetration depth of ogive-nose projectiles into concrete targets," *International Journal of Impact Engineering*, vol. 15, no. 4, pp. 395–405, 1994.

[72] Z.-C. Mu, *The Research on Penetration Characters of Concrete Material under Steel Penetrating Model*, Harbin Institute of Technology, Harbin, China, 2012, (Chinese).

[73] S. B. Segletes, "The erosion transition of tungsten-alloy long rods into aluminum targets," *International Journal of Solids and Structures*, vol. 44, no. 7-8, pp. 2168–2191, 2007.

[74] J.-F. Lou, *Theory Model and Numerical Simulation Research on Penetrating into Semi-Infinite Targets*, China Academy of Engineering Physics, Mianyang, China, 2012, (Chinese).

[75] R. F. Bishop, R. Hill, and N. F. Mott, "The theory of indentation and hardness tests," *Proceedings of the Physical Society*, vol. 57, no. 3, article 301, pp. 147–159, 1945.

[76] R. Hill, *The Mathematical Theory of Plasticity*, Oxford University Press, London, UK, 1950.

[77] Z. Rosenberg and E. Dekel, "Numerical study of the transition from rigid to eroding-rod penetration," *Journal de Physique Archives*, vol. 110, pp. 681–686, 2003.

[78] Z. Rosenberg and E. Dekel, "On the deep penetration of deforming long rods," *International Journal of Solids and Structures*, vol. 47, no. 2, pp. 238–250, 2010.

[79] A. Tate, "A possible explanation for the hydrodynamic transition in high speed impact," *International Journal of Mechanical Sciences*, vol. 19, no. 2, pp. 121–123, 1977.

[80] V. P. Alekseevskii, "Penetration of a rod into a target at high velocity," *Combustion, Explosion, and Shock Waves*, vol. 2, no. 2, pp. 63–66, 1969.

[81] F. F. Vitaman, N. A. Zlatin, and B. S. Loffe, "Deformable resistance of metals at velocities 10^{-6}-10^{2}m/s," *Journal of Technical Physics*, vol. 19, pp. 300–326, 1949.

[82] F. F. Vitman and N. A. Zlatin, "On collision of deformable bodies and its modeling. I," *Journal of Technical Physics*, vol. 33, pp. 982–989, 1963.

[83] L. V. Belyakov, F. F. Vitman, and N. A. Zlatin, "On collision of deformable bodies and its modeling. II," *Journal of Technical Physics*, vol. 33, pp. 990–995, 1963.

[84] N. A. Zlatin and G. I. Mishin, *Ballistic Ranges and Their Application in Experimental Research*, Nauka Press, Moscow, Russia, 1974.

[85] A. Tate, "Long rod penetration models—part I. A flow field model for high speed long rod penetration," *International Journal of Mechanical Sciences*, vol. 28, no. 8, pp. 535–548, 1986.

[86] A. Tate, "Long rod penetration models. Part II. Extensions to the hydrodynamic theory of penetration," *International Journal of Mechanical Sciences*, vol. 28, no. 9, pp. 599–612, 1986.

[87] G. C. Sun, J. Y. Wu, G. Z. Zhao et al., "A simplified model of long-rod projectile penetration of semi-infinite targets at normal incidence," *Acta Armamentarii*, vol. 3, pp. 1–8, 1981 (Chinese).

[88] Z. Rosenberg, E. Marmor, and M. Mayseless, "On the hydrodynamic theory of long-rod penetration," *International Journal of Impact Engineering*, vol. 10, no. 1–4, pp. 483–486, 1990.

[89] L.-S. Zhang and F.-L. Huang, "Model for long-rod penetration into semi-infinite targets," *Journal of Beijing Institute of Technology*, vol. 13, no. 3, pp. 285–289, 2004.

[90] C. E. Anderson Jr., J. D. Walker, S. J. Bless, and Y. Partom, "On the L/D effect for long-rod penetrators," *International Journal of Impact Engineering*, vol. 18, no. 3, pp. 247–264, 1996.

[91] B. Lan and H. Wen, "Alekseevskii-Tate revisited: an extension to the modified hydrodynamic theory of long rod penetration," *Science China Technological Sciences*, vol. 53, no. 5, pp. 1364–1373, 2010.

[92] H. Wen, Y. He, and B. Lan, "Analytical model for cratering of semi-infinite metallic targets by long rod penetrators," *Science China Technological Sciences*, vol. 53, no. 12, pp. 3189–3196, 2010.

[93] A. A. Kozhushko, A. D. Izotov, V. B. Lazarev et al., "Hydrodynamic model concepts in the problem of the dyanmic strength of materials of various physicochemica nature. II. Effets of

the strength characterisitics of media," *Neorganicheskie Materialy*, vol. 29, pp. 1189–1209, 1993.

[94] J. Zhao, X. W. Chen, F. N. Jin, and Y. Xu, "Depth of penetration of high-speed penetrator with including the effect of mass abrasion," *International Journal of Impact Engineering*, vol. 37, no. 9, pp. 971–979, 2010.

[95] S. A. Silling and M. J. Forrestal, "Mass loss from abrasion on ogive-nose steel projectiles that penetrate concrete targets," *International Journal of Impact Engineering*, vol. 34, no. 11, pp. 1814–1820, 2007.

[96] L.-L. He, X.-W. Chen, and X. He, "Parametric study on mass loss of penetrators," *Acta Mechanica Sinica*, vol. 26, no. 4, pp. 585–597, 2010.

[97] L.-L. He, *Dynamic Behavior Research on the Projectile Penetrating into Concrete with Considering Mass Losing and Nose Passivation*, China University of Sciences and Technology, Hefei, China, 2012 (Chinese).

[98] S. E. Jones, J. C. Foster, O. A. Toness et al., "An estimate for mass loss from high velocity steel penetrators," in *Proceedings of the ASME PVP-435 Conference on Thermal-Hydraulic Problems, Sloshing Phenomena, and Extreme Loads on Structures*, vol. 422, pp. 227–237, ASME, New York, NY, USA, 2002.

[99] L.-L. He and X.-W. Chen, "Analyses of the penetration process considering mass loss," *European Journal of Mechanics A/Solids*, vol. 30, no. 2, pp. 145–157, 2011.

[100] Y. Yang, *Problems Research on Penetration and Run Through of Concrete*, China University of Sciences and Technology, Hefei, China, 2012, (Chinese).

[101] H.-M. Wen and B. Lan, "Analytical models for the penetration of semi-infinite targets by rigid, deformable and erosive long rods," *Acta Mechanica Sinica*, vol. 26, no. 4, pp. 573–583, 2010.

[102] M. J. Forrestal and T. L. Warren, "Penetration equations for ogive-nose rods into aluminum targets," *International Journal of Impact Engineering*, vol. 35, no. 8, pp. 727–730, 2008.

[103] C.-B. Li, Z.-W. Shen, and M.-J. Pei, "Calculation analysis of rod-shaped projectile penetrating into concrete targets," *Journal of University of Science and Technoloty China*, vol. 28, pp. 215–219, 2008 (Chinese).

[104] J. Zhao, Y.-H. Zhao, J.-L. Shan et al., "The Hugoniot equation of state for Bukit Timah granite," *Chinese Journal of Geotechnical Engineering*, vol. 21, pp. 315–318, 1999 (Chinese).

[105] A. C. Charters and J. L. Summers, "Some comments on the phenomena of high speed impact," in *Proceedings of the Dicennial Symposium*, U.S. Naval Ordnance Laboratory, White Oak, Md, USA, 1959.

[106] R. J. Eichelberger, "Effects of meteoroid impacts on space vehicles," *ARS Journal*, vol. 32, no. 10, pp. 1583–1591, 1962.

[107] I. J. Loeffler, S. Liebleln, and N. Clough, "Meteoroid protection for space radiators, progress in astronautics and aeronautics," in *Power Systems for Space Flight*, M. A. Zipkin and R. N. Edwards, Eds., Academic Press, 1963.

[108] D. R. Christman and J. W. Gehring, "Analysis of high-velocity projectile penetration mechanics," *Journal of Applied Physics*, vol. 37, no. 4, pp. 1579–1587, 1966.

[109] J. M. Walsh and W. E. Johnson, "On the theory of hypervelocity impact," in *Proceedings of the 7th Symposium on Hypervelocity Impact*, Tampa, Fla, USA, 1964.

[110] E. L. Christiansen, "Design and performance equations for advanced meteoroid and debris shields," *International Journal of Impact Engineering*, vol. 14, no. 1–4, pp. 145–156, 1993.

[111] J.-S. Zhou, L. Zhen, and D.-Z. Yang, " Damage behaviors of several metal materials under impacts of projectiles with hypervelocities of 2.6~7 km/s," *Journal of Astronautics*, vol. 21, pp. 75–81, 2000 (Chinese).

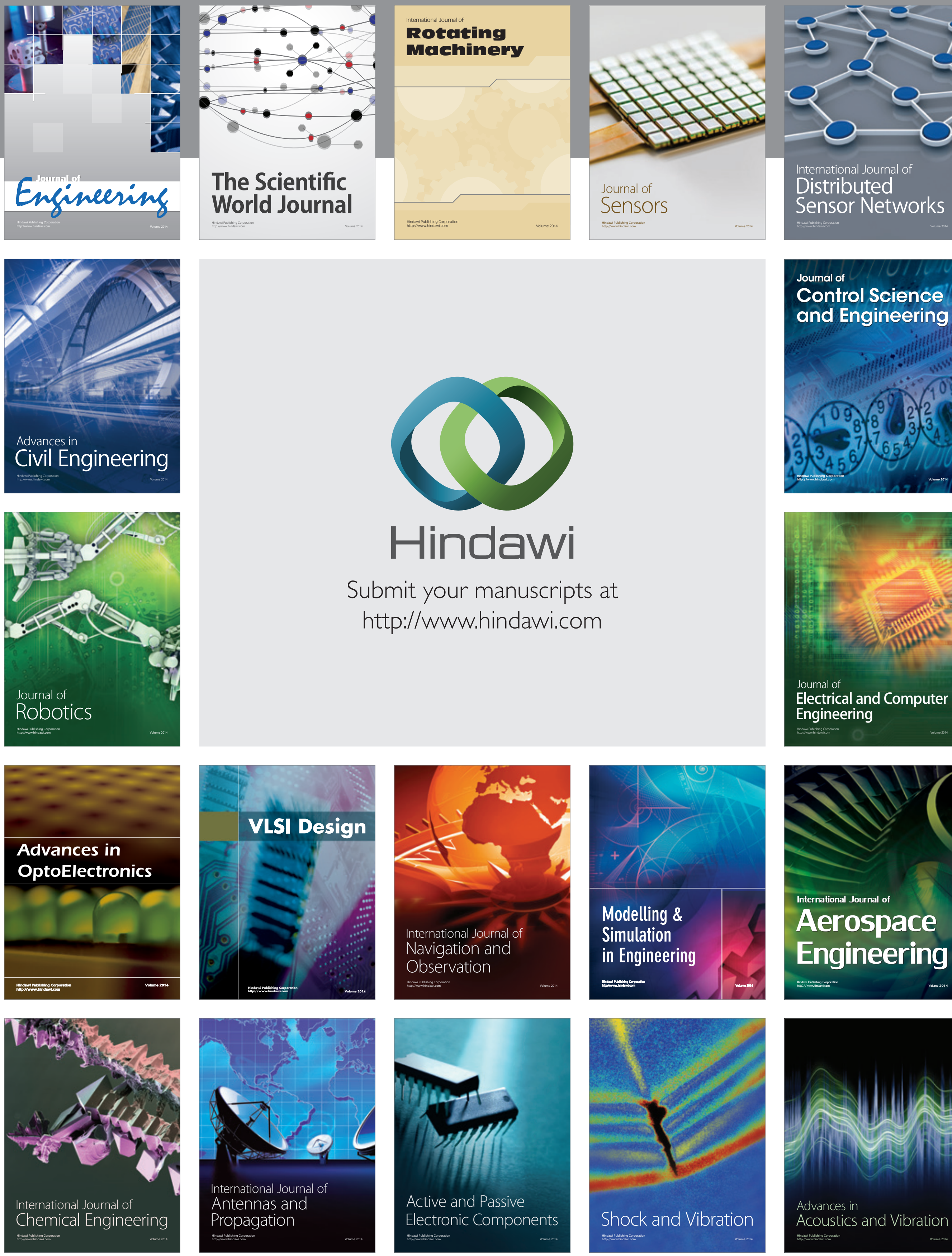
Journal of Engineering
The Scientific World Journal
International Journal of Rotating Machinery
Journal of Sensors
International Journal of Distributed Sensor Networks
Advances in Civil Engineering
Hindawi
Submit your manuscripts at
http://www.hindawi.com
Journal of Control Science and Engineering
Journal of Robotics
Journal of Electrical and Computer Engineering
Advances in OptoElectronics
VLSI Design
International Journal of Navigation and Observation
Modelling & Simulation in Engineering
International Journal of Aerospace Engineering
International Journal of Chemical Engineering
International Journal of Antennas and Propagation
Active and Passive Electronic Components
Shock and Vibration
Advances in Acoustics and Vibration